Quantifying the influence of sea ice on ocean microseism using observations from the Bering Sea, Alaska

Victor C. Tsai[1,2] and Daniel E. McNamara[2]

Received 23 September 2011; revised 21 October 2011; accepted 23 October 2011; published 19 November 2011.

[1] Microseism is potentially affected by all processes that alter ocean wave heights. Because strong sea ice prevents large ocean waves from forming, sea ice can therefore significantly affect microseism amplitudes. Here we show that this link between sea ice and microseism is not only a robust one but can be quantified. In particular, we show that 75–90% of the variability in microseism power in the Bering Sea can be predicted using a fairly crude model of microseism damping by sea ice. The success of this simple parameterization suggests that an even stronger link can be established between the mechanical strength of sea ice and microseism power, and that microseism can eventually be used to monitor the strength of sea ice, a quantity that is not as easily observed through other means. **Citation:** Tsai, V. C., and D. E. McNamara (2011), Quantifying the influence of sea ice on ocean microseism using observations from the Bering Sea, Alaska, *Geophys. Res. Lett.*, *38*, L22502, doi:10.1029/2011GL049791.

1. Introduction

[2] Ambient seismic noise is relatively well characterized [*McNamara and Buland*, 2004; *Berger et al.*, 2004]. It is well known that within the 1 s to 20 s period band, there are two major peaks in the noise spectrum due to secondary (≈1 s to 10 s) and primary (≈10 s to 20 s) ocean microseism [*McNamara and Buland*, 2004]. Ocean microseism is known to be generated by ocean-wave energy being converted into seismic energy through either the direct impact of the waves upon shorelines or the generation of pressure perturbations on the ocean floor [*Longuet-Higgins*, 1950; *Hasselmann*, 1963; *Tanimoto*, 2007]. However, there remains some disagreement regarding the relative importance of deep-water versus shallow-water excitation of secondary microseism [*Bromirski and Duennebier*, 2002; *Bromirski et al.*, 2005; *Kedar et al.*, 2008].

[3] Due to this understanding, there are a number of features of microseism that are somewhat predictable. For example, it is known that microseism amplitudes observed on land generally decrease as a function of distance from coastlines (with shorter periods being attenuated faster) and exhibit a seasonality that is due to the seasonal presence or absence of large storms (and hence the occurrence of large waves) [*McNamara and Buland*, 2004; *Schulte-Pelkum et al.*, 2004; *Stehly et al.*, 2006; *Gerstoft and Tanimoto*, 2007; *Gerstoft et al.*, 2008]. Moreover, microseism amplitudes are known to be affected by processes that affect ocean wave heights. For example, changes in climate that result in larger or more energetic storms have a significant effect on microseism variability [*Aster et al.*, 2008, 2010].

[4] It has also been observed that sea ice formation around Antarctica causes a local reduction in microseism amplitudes [*Cathles et al.*, 2009; *Stutzmann et al.*, 2009; *Grob et al.*, 2011]. This effect of sea ice attenuating ocean microseism is the topic of our current study. We make two primary contributions. First, we document observations of a sea ice microseism signal at near-coastal stations bordering the Bering Sea (Alaska). Secondly, we use these observations to quantify how strongly sea ice affects microseism. The goal of this work is to show that it is possible to establish a quantitative relationship between sea ice properties and microseism amplitudes at various frequencies, with the implication that we may eventually be able to use microseism variability to estimate mechanical properties of sea ice that are difficult to constrain through other observations. Moreover, better quantification of this sea ice effect may yield important constraints on the extent to which deep-water excitation is a significant source of secondary microseism.

2. Data

[5] We use seismic data from 3 stations of the Alaska Regional Seismic Network within the Bering Sea. From south to north, these are UNV (Unalaska Valley, 53.85°N, 166.50°W), GAMB (Gambell, 63.78°N, 171.70°W), and TNA (Tin City, Alaska, 65.56°N, 167.92°W) (see triangles in Figure 1). UNV is situated on Unalaska Island in the Aleutian Islands at the southern extent of the Bering Sea, south of the most southerly extent of sea ice, and will be used as a reference station that is unaffected by sea ice. GAMB is on St. Lawrence Island in the middle of the Bering Sea, and TNA is near the tip of the Seward Peninsula, adjacent to the Bering Strait and at the northern extent of the Bering Sea. Both GAMB and TNA are surrounded by sea ice roughly between Dec and May of each year. Continuous data from Oct 2002–May 2010 were processed to obtain hourly average power spectral densities (PSDs) in various period bands, ranging from 0.1–10 s [*McNamara and Buland*, 2004]. These PSDs form the basis for this study. It may be noted that these 3 stations represent the only stations bordering the Bering Sea with at least 7 years of nearly continuous, mostly glitch-free data.

[6] Sea ice concentration data were obtained from the biweekly analysis product of the National Ice Center (NIC, accessible from http://www.natice.noaa.gov/products), which is operated jointly by the National Oceanic and Atmospheric Administration (NOAA), the U.S. Navy and the

[1]Seismological Laboratory, California Institute of Technology, Pasadena, California, USA.
[2]Geologic Hazards Science Center, U.S. Geological Survey, Golden, Colorado, USA.

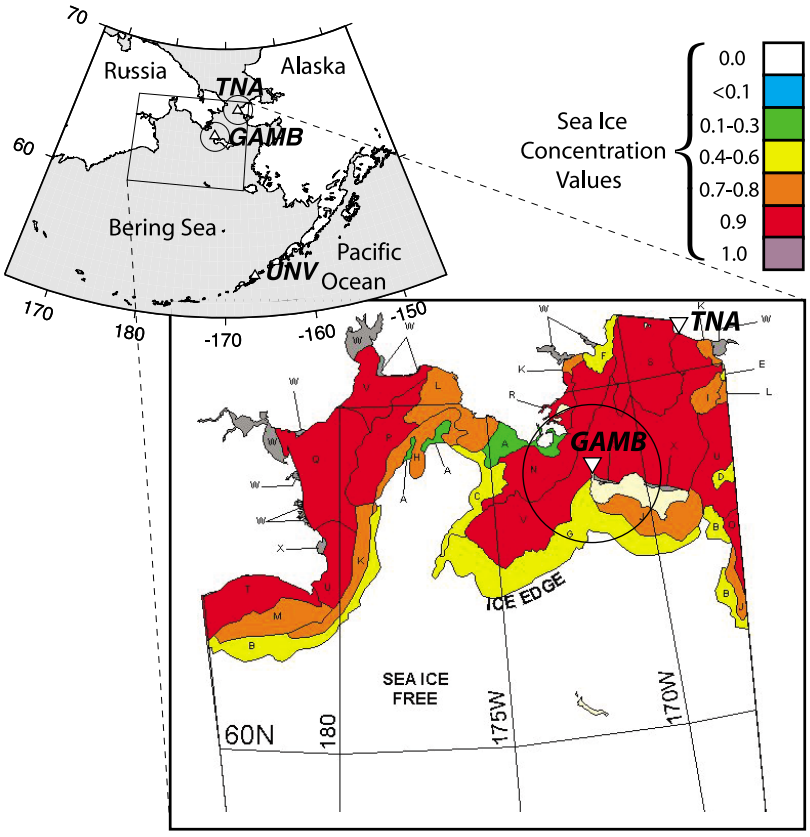

Figure 1. Map of sea ice concentration on 17 Dec 2004 from the National Ice Center (http://www.natice.noaa.gov) with seismic stations shown as triangles and 100 km-radius circles drawn around GAMB and TNA (in inset). Colors denote different sea ice concentrations, with gray = 1.0, red = 0.9, orange = 0.7–0.8, yellow = 0.4–0.6, green = 0.1–0.3, blue <0.1, and white = ice free (or land). Letters denote different sea ice types (and are not used in this study).

U.S. Coast Guard. A typical concentration map is shown in Figure 1, with sea ice concentration being color coded in 7 different bins. Sea ice concentration is estimated primarily from satellite observations of the differences in spectral characteristics of sea ice and sea water. We note that similar products are available through other sources like the National Sea Ice Data Center (http://nsidc.org); we choose the NIC dataset for this study because of the higher spatial resolution provided.

3. Analysis

3.1. Spectrograms

[7] In Figure 2, we plot spectrograms for UNV, TNA and GAMB covering the time period from Nov 2002 to Jul 2008

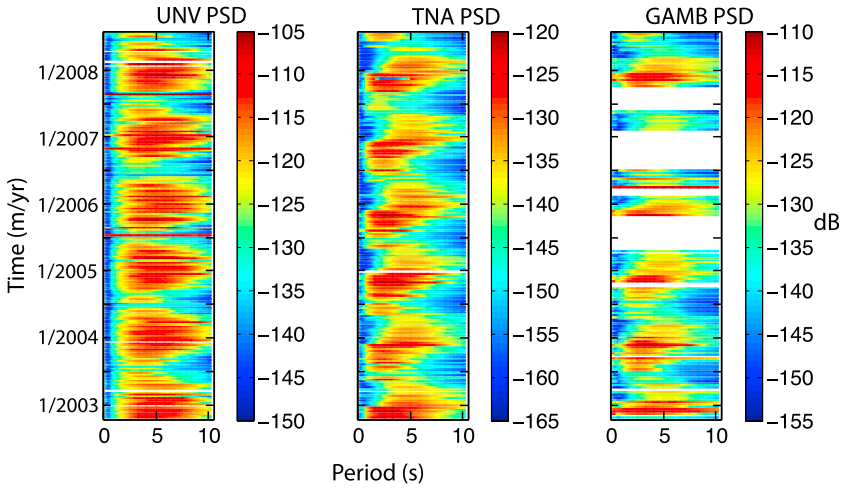

Figure 2. Power spectral density (PSD) as a function of time (y axis) and period (x axis) for stations UNV, TNA and GAMB. Color scale is in dB (with respect to acceleration power, which has units of $(m/s^2)^2/Hz$). Data gaps appear white.

and period ranging from 0.1 s to 10 s. Although all three stations have some data gaps and glitches (including sensor malfunction and telemetry problems), with GAMB having at least 5 notable gaps, it is relatively straightforward to interpret the remainder of the time series.

[8] Since station UNV is unaffected by sea ice, the PSD variability seen here is typical of seasonal ocean microseism variability. In particular, the seasonal increase in microseism power that corresponds with the presence of large winter storms is clearly visible. Although there is spatial variability to the ocean microseism signal [*McNamara and Buland*, 2004], all near-coastal seismic stations surrounding the northern Pacific have a similar dependence on ocean microseism and UNV will be used as a proxy for this 'north Pacific' ocean microseism signal. We further note that, as for most near-coastal stations that are relatively far away from highly populated areas, secondary microseism is observed down to periods of well below 2 s, in this case with significant power (above −130 dB) down to at least 0.5 s.

[9] Comparing the TNA and GAMB spectrograms with that of UNV, there are a number of similarities and a few notable differences. Except for glitches, the main seasonal trend of north Pacific microseism is again present, with generally higher power in the winter months. However, the absolute level of microseism power is substantially lower at TNA compared to UNV and GAMB also has slightly lower microseism power (note the different color scales in Figure 2). This difference in absolute power can be understood as primarily being due to the average distance of each of the stations to the main Pacific storm activity (TNA is farthest north, GAMB is intermediate, and UNV is farthest south, and closest to the main storm tracks in the Pacific). This distance then results in lower local wind speeds (and hence lower local wave heights), and also results in attenuation of the largest storm waves prior to their being observed at each station.

[10] In addition to the difference in absolute power is the dramatic loss of microseism power in the ≈0.1–3 s period band in the months of December-May for both TNA and GAMB relative to UNV. This drop in signal is extremely clear in all years for which continuous data exist, and cannot be attributed to any behavior seen by UNV. Moreover, for the 3 years for which both TNA and GAMB have mostly continuous data (winters of '02–'03, '03–'04 and '07–'08), the drop in signal is seen more prominently and more extensively by TNA compared to GAMB. Since sea ice begins forming in the Bering Sea in December and begins to recede in May, these observations strongly suggest that sea ice wave damping causes this variability. The remainder of this work will be spent quantifying the expected effect of sea ice on microseism and showing that a simple model of this effect accurately predicts the observed decrease in short-period microseism. We focus on the short-period portion of microseism power centered at 1 s period and averaged across 2 octaves (0.6–2.0 s period).

3.2. A Model for Sea Ice Microseism Variability

[11] In this preliminary analysis, we construct a crude parameterization of sea ice strength that allows us to show that short-period microseism amplitudes are strongly affected by sea ice to the extent that most of the variability described in the previous section can be explained by this model. As will be seen, the parameterized model does not attempt to fully describe the physics of the system, but rather simplifies the physics into just a few key parameters. The two main ideas of the model are that (1) short-period microseism is locally generated, since microseism that is generated farther away would be highly attenuated and not observed, and (2) strong sea ice prevents large ocean waves from existing and hence dampens the generation of 0.1–3 s microseism. We note that this dampening may be related to both wave generation and maintaining these waves.

[12] Throughout this work, we define sea ice (mechanical) strength in terms of how strongly sea ice is able to decrease the amplitude of ocean waves (and thus affect microseism amplitudes). For a purely elastic material, this definition of strength would be monotonically related to an averaged stiffness, while for a viscous material, strength would be monotonically related to an averaged viscosity. Since sea ice is neither purely elastic nor purely viscous, strength is related to both quantities and averaged appropriately. Here, we do not attempt to describe a physical model for strength but simply use strength to define the effect of sea ice on microseism amplitudes.

[13] To approximately account for the first main idea, in the parameterized model we assume that the seismic stations are only affected by sea ice within a certain attenuation length, L. *Prieto et al.* [2009] suggest that attenuation coefficients at 1 s period could potentially be around 10^{-2}/km, giving an attenuation length of $L \approx 100$ km. This is consistent with estimates of Q in the continental U.S. [*Erickson et al.*, 2004]. While such continental estimates may not strictly be appropriate for the Bering Sea region, it is at least a useful first estimate. We then assume that the 1-s microseism is affected only by sea ice within a circular area of radius L from the station (see Figure 1). For GAMB, on St. Lawrence Island, this area extends to the nearest Russian coastline; for TNA, this area includes part of the Chukchi Sea (north of the Bering Strait). In reality, we expect there to be a gradual decrease in sensitivity due to attenuation, instead of an abrupt cutoff at 100 km, but in this first attempt at characterization, an abrupt cutoff at 100 km is thought to be a decent approximation.

[14] To account for the second main idea, we assume that average sea ice concentration is an adequate proxy for sea ice strength, and hence that sea ice concentration is a good predictor of a decrease in microseism power. With this assumption, we can use the sea ice concentration biweekly analysis dataset as described above (see Figure 1) to yield a model variable. Concentrations in the biweekly analysis are given in 7 concentration bins, and we use the following concentration values for those bins: 1.0 for gray, 0.9 for red, 0.7 for orange, 0.5 for yellow, 0.2 for green, 0.1 for blue, and 0.0 for white. To construct our proxy for sea ice strength, $S_i(t)$, at each station i, we then linearly average the concentration values over the area in question (as described in the previous paragraph). For example, in Figure 1, $S_{\mathrm{GAMB}} = 0.78$. S_{TNA} includes area from the Chukchi Sea (not shown), but for the subset of the area within the Bering Sea, $S_{\mathrm{TNA}} = 0.87$.

[15] With S_i defined, we now define our parameterized model. As described in Section 3.1, each station has a variability due to typical microseism variability from the presence or absence of large storms, which affect wave heights over a relatively large areal extent. To account for

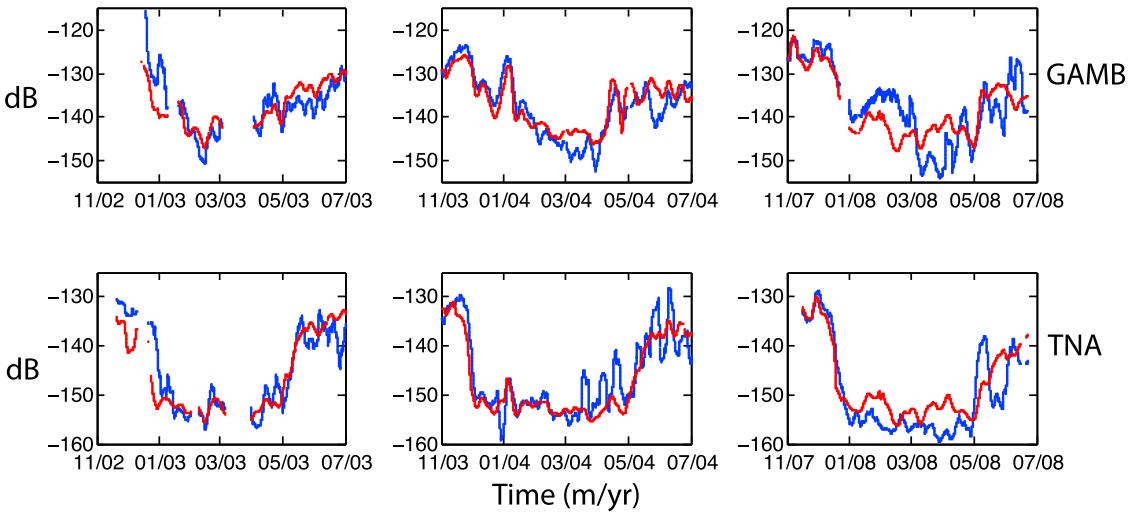

Figure 3. Observed (blue) versus modeled (red) microseism power (in dB relative to acceleration power) averaged across period range 0.6–2.0 s. The red curves are best-fit curves to the 3-parameter model described by equation (1). Time periods with glitches are removed from the data and not used in constructing the model curves. First row is for GAMB over three seasons, second row is for TNA for the same three seasons.

this (including the difference in absolute power), we assume that the first order variability in seismic power at each station is simply a scaled version of the variability observed at reference station UNV, with a possible offset in absolute power. That is, we take the PSD observed at station i to be linearly related to the PSD observed at UNV. With our crude parameterization of average local sea ice strength given by $S_i(t)$ (as a function of time, t), we further assume that the PSD (in dB) observed at each station, $P_i(t)$, is linearly related to $S_i(t)$. It is expected that the scaling coefficient is negative, meaning that an increase in sea ice strength directly causes a decrease in wave heights and therefore leads to a decrease in microseism power. This two-component model can then be written as

$$P_i(t) = C_{i0} + C_{i1} \cdot P_{\mathrm{UNV}}(t) + C_{i2} \cdot S_i(t) \qquad (1)$$

where C_{ij} are three coefficients to be determined for each station, i. Both C_{i0} and C_{i1} are expected to be smaller (or more negative) for stations farther away from the main microseism generating regions of the Pacific Ocean since this distance affects both the average microseism level (C_{i0}) and the relative amplitude of microseism variations (C_{i1}). C_{i2}, on the other hand, represents how strongly local sea ice strength (concentration) affects local microseism and can therefore be expected to be roughly constant between coastal stations.

3.3. Model Fits to Observed Data

[16] Using the simple two-component (3 parameter) model of equation (1), we solve for best-fit coefficients C_{ij} using continuous data from the 3 seasons for which the seismic data is mostly glitch-free (winters of '02–'03, '03–'04 and '07–'08). Even these 3 seasons are not completely glitch-free, and we further remove time periods for which glitches are known to exist. Using the remainder of the three-season time series as data, $\boldsymbol{d} \equiv P_i(t)$, we solve for the model vector $\boldsymbol{m} \equiv [C_{i0}C_{i1}C_{i2}]^T$ by least squares inversion. Since the sea ice data are only provided biweekly, these data are interpolated onto the seismic hourly PSD time series. The resulting regression coefficients are listed in Table 1 and the model prediction is plotted against the observed data in Figure 3. The correlation coefficients for TNA and GAMB are $r_{\mathrm{TNA}} = 0.882$ and $r_{\mathrm{GAMB}} = 0.798$.

[17] In addition to the high correlation coefficients, visual inspection of Figure 3 shows that most of the observed variability in the TNA and GAMB PSDs are explainable with the simple model proposed above. In particular, most of the short-timescale (weekly) as well as long-timescale (monthly) variability is well captured by the model. There are, however, some notable features that are not well captured. For example, the drop in microseism power at TNA in the '02–'03 season occurs nearly one month earlier in the model compared to the observations, the average trend in the Feb-Mar '08 GAMB record is not well fit, and a spike exists in May '08 of the TNA observations whose amplitude is not well captured by the model. Yet despite these discrepancies, and despite the simplicity of the model, the fits are surprisingly good. In particular, the model demonstrates that the first-order variability in microseism power in the Bering Sea is clearly due to damping by sea ice (with more damping with stronger sea ice). One may note that the regression coefficients C_{i2} are close to −20 for both TNA and GAMB (−23 and −17 respectively), suggesting that $C_{i2} \approx -20$ may be appropriate as a global constant to scale between locally averaged sea ice concentrations and microseism power (in dB) at coastal locations.

4. Discussion and Conclusions

[18] In previous sections, we show that a simple model for sea ice strength (see equation (1)) explains 75–90% of the variability observed in short-period (1 s) Bering Sea

Table 1. Linear Regression Coefficients

	C_{i0}	C_{i1}	C_{i2}
TNA	−24.516	0.8314	−23.438
GAMB	17.932	1.1305	−17.329

microseism PSDs. This good predictability suggests that a strong link can be made between 0.1–3 s microseism power and sea ice strength (in areas affected by seasonal sea ice cover).

[19] However, a number of issues should be addressed before predictability will be robust. First, a more physically-based parameterization than used here may be necessary for more accurate prediction. For example, it is possible that the disagreement in the timing of the '02–'03 drop in microseism power at TNA is due to the approximate regionalization done here that could potentially be improved to account for a smoothly varying sensitivity to local sea ice. On the other hand, some of this disagreement may also be because sea ice concentration is not an accurate predictor of sea ice strength (and that microseism power may be a better predictor); in this case, modeling could be improved by utilizing a physical model to relate sea ice strength with observed seismic power. The disagreement may also be partly due to the use of UNV as a proxy for microseism strength, even though UNV is hundreds of km away from TNA (and GAMB). A second related problem is that we have assumed microseism to be equally sensitive to all sea ice within radius L, whereas there is a dependence of microseism generation on ocean depth such that near-shore waves (and hence sea ice) could be more important than off-shore waves [*Longuet-Higgins*, 1950; *Bromirski and Duennebier*, 2002; *Tanimoto*, 2007; *Kedar et al.*, 2008]. Preliminary tests show that our model is not very sensitive to this issue, but further testing is necessary. A final problem is that in order for such predictions to be made robustly, the relevant seismic stations need to operate continuously and with limited glitches. This is especially problematic for distant stations in the Arctic that often have telemetry issues and are also not easily accessible for repairs.

[20] Despite the potential problems discussed, the very good quantitative agreement between the simple model of sea-ice modulated microseism proposed here and the observed microseism suggests that microseism can be used to predict the strength of sea ice, a property that is not easily observed through other means. In particular, it may be possible that using observed microseism variability to predict local mechanical strength of sea ice can be more accurate than using satellite observations of sea ice concentration to infer sea ice strength. Being able to predict sea ice mechanical strength would be useful on a number of different levels, including knowing how close this ice is to disintegrating. Such knowledge could potentially be useful for the shipping industry as well as climate scientists.

[21] **Acknowledgments.** The authors thank A. T. Ringler, S. O'Neel, F. Walter, P. D. Bromirski, V. Schlindwein, and S. Kedar for helpful comments. We also thank the Alaska Earthquake Information Center and the National Ice Center for providing the data used. This research was supported by the Mendenhall Postdoctoral Fellowship program of the United States Geological Survey.

[22] The Editor thanks two anonymous reviewers for their assistance in evaluating this paper.

References

Aster, R. C., D. E. McNamara, and P. D. Bromirski (2008), Multidecadal climate-induced variability in microseisms, *Seismol. Res. Lett.*, *79*, 194–202.

Aster, R. C., D. E. McNamara, and P. D. Bromirski (2010), Global trends in extremal microseism intensity, *Geophys. Res. Lett.*, *37*, L14303, doi:10.1029/2010GL043472.

Berger, J., P. Davis, and G. Ekström (2004), Ambient Earth noise: A survey of the Global Seismographic Network, *J. Geophys. Res.*, *109*, B11307, doi:10.1029/2004JB003408.

Bromirski, P. D., and F. K. Duennebier (2002), The near-coastal microseism spectrum: Spatial and temporal wave climate relationships, *J. Geophys. Res.*, *107*(B8), 2166, doi:10.1029/2001JB000265.

Bromirski, P. D., F. K. Duennebier, and R. A. Stephen (2005), Mid-ocean microseisms, *Geochem. Geophys. Geosyst.*, *6*, Q04009, doi:10.1029/2004GC000768.

Cathles, L. M., IV, E. A. Okal, and D. R. MacAyeal (2009), Seismic observations of sea swell on the floating Ross Ice Shelf, Antarctica, *J. Geophys. Res.*, *114*, F02015, doi:10.1029/2007JF000934.

Erickson, D., D. E. McNamara, and H. M. Benz (2004), Frequency-dependent Lg Q within the continental United States, *Bull. Seismol. Soc. Am.*, *94*, 1630–1643.

Gerstoft, P., and T. Tanimoto (2007), A year of microseisms in Southern California, *Geophys. Res. Lett.*, *34*, L20304, doi:10.1029/2007GL031091.

Gerstoft, P., P. M. Shearer, N. Harmon, and J. Zhang (2008), Global P, PP, and PKP wave microseisms observed from distant storms, *Geophys. Res. Lett.*, *35*, L23306, doi:10.1029/2008GL036111.

Grob, M., A. Maggi, and E. Stutzmann (2011), Observations of the seasonality of the Antarctic microseismic signal, and its association to sea ice variability, *Geophys. Res. Lett.*, *38*, L11302, doi:10.1029/2011GL047525.

Hasselmann, K. (1963), A statistical analysis of the generation of microseisms, *Rev. Geophys.*, *1*, 177–210.

Kedar, S., M. Longuet-Higgins, F. Webb, N. Graham, R. Clayton, and C. Jones (2008), The origin of deep ocean microseisms in the North Atlantic Ocean, *Proc. R. Soc. A*, *464*, 777–793.

Longuet-Higgins, M. S. (1950), A theory of the origin of microseisms, *Philos. Trans. R. Soc. A*, *243*, 1–35.

McNamara, D. E., and R. P. Buland (2004), Ambient noise levels in the continental United States, *Bull. Seismol. Soc. Am.*, *94*, 1517–1527.

Prieto, G. A., J. F. Lawrence, and G. C. Beroza (2009), Anelastic Earth structure from the coherency of the ambient seismic field, *J. Geophys. Res.*, *114*, B07303, doi:10.1029/2008JB006067.

Schulte-Pelkum, V., P. S. Earle, and F. L. Vernon (2004), Strong directivity of ocean-generated seismic noise, *Geochem. Geophys. Geosyst.*, *5*, Q03004, doi:10.1029/2003GC000520.

Stehly, L., M. Campillo, and N. M. Shapiro (2006), A study of the seismic noise from its long-range correlation properties, *J. Geophys. Res.*, *111*, B10306, doi:10.1029/2005JB004237.

Stutzmann, E., M. Schimmel, G. Patau, and A. Maggi (2009), Global climate imprint on seismic noise, *Geochem. Geophys. Geosyst.*, *10*, Q11004, doi:10.1029/2009GC002619.

Tanimoto, T. (2007), Excitation of microseisms, *Geophys. Res. Lett.*, *34*, L05308, doi:10.1029/2006GL029046.

D. E. McNamara, Geologic Hazards Science Center, U.S. Geological Survey, 1711 Illinois St., Golden, CO 80403, USA. (mcnamara@usgs.gov)

V. C. Tsai, Seismological Laboratory, California Institute of Technology, 1200 E. California Blvd., Pasadena, CA 91125, USA. (tsai@caltech.edu)